Structure Comparison between Oxidized and Reduced Plastocyanin from a Fern, *Dryopteris crassirhizoma*[†,‡]

Tsuyoshi Inoue,[§] Masaharu Gotowda,[§] Hajime Sugawara,[§] Takamitsu Kohzuma,[||] Fuminori Yoshizaki,[⊥] Yasutomo Sugimura,[⊥] and Yasushi Kai*[,§]

Department of Materials Chemistry, Graduate School of Engineering, Osaka University, Suita, Osaka, Japan, Department of Biochemistry, Faculty of Science, Ibaraki University, Mito, Ibaraki, Japan, and Faculty of Science, Toho University, Funabashi, Chiba, Japan

Received March 3, 1999; Revised Manuscript Received July 20, 1999

ABSTRACT: The X-ray crystal structures of oxidized and reduced plastocyanin obtained from the fern *Dryopteris crassirhizoma* have been determined at 1.7 and 1.8 Å resolution, respectively. The fern plastocyanin is unique in the longer main chain composed of 102 amino acid residues and in the unusual pH dependence due to the $\pi-\pi$ stacking interaction around the copper site [Kohzuma, T., et al. (1999) *J. Biol. Chem. 274*, 11817−11823]. Here we report the structural comparison between the fern plastocyanin and other plastocyanins from cyanobacteria, green algae, and other higher plants, together with the structural changes of fern plastocyanin upon reduction. Glu59 hydrogen bonds to the OH of Tyr83, which is thought to be a possible conduit for electrons, in the oxidized state. However, it moves away from Tyr83 upon reduction like poplar plastocyanin.

Plastocyanin is a small (91−105 amino acids) copper-binding protein, which functions as a shuttle for electron transfer from cytochrome *f* of the b_6f complex to $P700^+$ of photosystem I in chloroplasts of algae and higher plants, and also in many cyanobacteria (*1*−*3*). Plastocyanin is the sole protein responsible for this task in the photosynthetic electron transfer system in higher plants. However, algae and cyanobacteria lacking plastocyanin use cytochrome c_6, previously also called cytochrome *c*-552 or *c*-553, to transport electrons from cytochrome *f* to $P700^+$ (*4*). Some organisms contain the genetic information for both plastocyanin and cytochrome c_6. In these organisms, the level of copper in the growth medium determines which gene is utilized (*5*−*9*).

The crystal and solution structures of plastocyanins from a number of higher plants and eukaryotic algae have been determined (*10*−*20*). Recently, three structures of plastocyanins from cyanobacteria were reported (*21*−*23*). One is that of plastocyanin from *Anabaena variabilis* which is comprised of 105 amino acid residues (*21*), and another is a triple mutant of the plastocyanin from *Synechocystis* sp. PCC 6803 which is comprised of 98 amino acid residues (*22*). The last one is plastocyanin from *Synechococcus* sp. PCC 7942 (*23*), and it is comprised of 91 amino acid residues. Despite the sequence divergence among plastocyanins from cyanobacteria, algae, and higher plants, their three-dimensional structures are remarkably similar. The overall topology of plastocyanin consists of an eight-stranded β-barrel structure made up of two β-sheets that resembles the known structures of other blue copper proteins such as azurin, amicyanin, and pseudoazurin. Plastocyanins from higher plants and green algae generally have a short (one-turn) α-helix from residues 52 to 55 between the two β-sheets (*3*). However, the crystal structure of plastocyanin from *Synechococcus* sp. PCC 7942 has a short 3_{10}-helix from Pro53 to Leu55 (*23*). The other cyanobacterial plastocyanins contain a slightly longer (two-turn) α-helix from residues 47 to 54 (*21*, *22*). Insertions and deletions occur around Gly49 and cause the local structural changes. The primary structure of *Dryopteris crassirhizoma* plastocyanin shows that it has insertions of three residues at positions 45A, 47A, and 47B, relative to the higher-plant protein (*24*), resulting in a protein with 102 amino acid residues. The protein is the longest known to date among higher-plant plastocyanins. The greatest degree of identity among plastocyanins is 40% (41/102) conservation of amino acid residues between *Dryopteris* and a green alga, *Ulva pertusa*, but only 35% (36/102) between *Dryopteris* and poplar, both of which are vascular plants.

The copper atom of plastocyanin is located in the northern end of the protein and is coordinated by two histidines (His37 and His87, the latter has a solvent-exposed imidazole ring), a methionine (Met92), and a cysteine (Cys84). The geometry of the active site is that of an irregular, or distorted, tetrahedron. The electron transfer kinetics of plastocyanins

[†]This work was supported by Grants-in-Aid for Scientific Research on Priority Areas 09261223 and 09235202 and Grants-in-Aid for Encouragement of Young Scientists 09780632 and 11780495 from the Ministry of Education, Science, Sports and Culture of Japan. This work was partially supported by Grants for Scientific Research from The Foundation for the Promotion of Industrial Science (to T.I.) and by Grants-in-Aid for the Ground Experiment for the Space Utilization from the Japan Space Forum and National Space Developments Agency of Japan (to T.K.). We are also grateful to the Sakabe project of the TARA (Tsukuba Advanced Research Alliance) center at the University of Tsukuba.

[‡]Atomic coordinates have been deposited in the Brookhaven Protein Data Bank under file names 1KDJ and 1KDI.

* To whom correspondence should be addressed. Telephone: +81-6-6879-7408. Fax: +81-6-6879-7409. E-mail: kai@chem.eng.osaka-u.ac.jp.

[§] Osaka University.

[||] Ibaraki University.

[⊥] Toho University.

10.1021/bi990502t CCC: $18.00
Published on Web 10/01/1999

have been investigated in detail, and two distinct surface patches for docking with physiological redox partners have been proposed (*2*, *25*, *26*). One is the hydrophobic patch around the solvent-exposed His87, and the other is the negatively charged acidic patch around Tyr83, which is thought to be a possible conduit for electrons, located on the east side of the molecule. The latter consists of two acidic clusters from residues 42 to 44 and 59 to 61 in higher-plant plastocyanins. In the algal plastocyanins, residues 58 and 59 are deleted but negatively charged residues not present in poplar are present at positions 53 and 85. The cyanobacteria plastocyanins apparently lack the mostly conserved acidic patch. Although the protein has only two acidic residues, Glu42 and Glu85, around Tyr83, these are neutralized by Arg88 and Lys58 (*22*, *23*). *Dryopteris* plastocyanin conserved the acidic residues at position 42 and 59; however, the other acidic residues at the acidic clusters are not conserved. The highly conserved Tyr83 is located on the east side of the molecule and is ca. 15 Å away from the copper atom. Both patches have been considered to be the essential electron transfer sites on the basis of kinetic studies (*27*, *28*).

The structure of the copper-binding site of oxidized poplar plastocyanin at pH 6.0 is almost identical to that of the reduced poplar plastocyanin at pH 7.8, with the largest deviation being 0.15 Å in the length of the Cu−$N_{\delta1}$(His87) bond (*12*). A remarkable change at the reduced copper center is observed at low pH values (*12*). The $N_{\delta1}$(His87) of the reduced protein becomes protonated with decreasing pH and moves slightly up and away from the copper atom, whereas the copper atom moves down and away from His87 so that it is eventually only trigonally coordinated by His37, Cys84, and Met92. At pH 5.1, the copper atom and its three liganding atoms are essentially coplanar, the $N_{\delta1}$(His87) is protonated, and the imidazole ring rotates about the C_β−C_γ bond. The distance between this nitrogen atom and the copper atom has increased to 3.05 Å (*3*, *12*). A similar effect has also been observed in crystallographic studies with pseudoazurin and amicyanin (*29*, *30*).

In this study, the X-ray structural analyses of the fern plastocyanin from *D. crassirhizoma* have been performed in both of the oxidized and reduced states at pH 4.5. We have already reported the active site structure of *Dryopteris* plastocyanin with pH resistance, unexpected absorption spectra, high redox potential, and remarkable activity for electron transport at low pH (*24*). Recently, we have succeeded in determining the structures of plastocyanins from the higher plant *Silene pratensis* (*19*), the green alga *U. pertusa* (*20*), and the cyanobacterium *Synechococcus* sp. PCC 7942 (*23*). We describe here not only the structural comparison among plastocyanins from higher plants, green algae, and cyanobacteria but also the structural comparison of the two forms at pH 4.5.

MATERIALS AND METHODS

Data Collection and Processing. The crystallization and data collection of oxidized and reduced plastocyanin from *D. crassirhizoma* were reported previously (*24*). The crystals belong to hexagonal space group $P6_1$ with the following unit cell parameters: $a = b = 73.15$ Å, and $c = 31.10$ Å. A set of intensity data for the oxidized form was collected with synchrotron radiation at the Photon Factory using Sakabe's Weissenberg camera for macromolecules (*31*). Among 69 003 accepted observations up to 1.7 Å resolution, 10 220 independent reflections were obtained with an R_{merge} of 8.9% and a completeness of 95.7%. The reduced form is prepared by the soaking method with the solution containing 10 mM sodium ascorbate. An intensity data set for the reduced form was collected up to 1.8 Å resolution on a Rigaku RAXIS-IIc imaging pate using CuKα radiation from a rotating anode X-ray generator (Rigaku RU-300) with a fine-focused beam and β-filtered (40 kV, 100 mA). Among 28 202 accepted observations up to 1.8 Å resolution, 8478 independent reflections were obtained with an R_{merge} of 6.1% and a completeness of 93.5%. All intensity data were processed using *DENZO* and scaled with the program *SCALEPACK* (*32*).

Structure Analysis and Refinement. The crystal structure of the oxidized form was determined by the molecular replacement method with the program of *AMORE* (*33*) in the *CCP4* program package (*34*). The molecular structure of plastocyanin from poplar was used as the starting model (PDB file name 1PCY) (*35*). The ratio of the identical to total residues is 36/102 (35%) between *Dryopteris* and poplar. The rotation function parameters were as follows: $\alpha = 39.54$, $\beta = 17.53$, and $\gamma = 108.68$; the translation parameters were as follows: $x = 0.732$, $y = 0.132$, and $z = 0$. The *R*-factor for the model structure was calculated to be 47% for 8−4 Å data.

Refinement of the oxidized structure was carried out at 1.7 Å resolution by the simulated annealing refinement method (*X-PLOR*; *38*). Model rebuilding was performed with the program *TURBO-FRODO* (*36*) by using Fourier maps calculated with coefficients of $(2F_o - F_c)\exp(2\pi i\alpha_{calc})$ and $(F_o - F_c)\exp(2\pi i\alpha_{calc})$ and an omit map. Ordered water molecules were included by selecting the peaks based on $F_o - F_c$ difference Fourier maps contoured at 2.5σ and $2F_o - F_c$ maps contoured at 1.2σ. The quality of the final model was assessed from Ramachandran plots (*38*), and the analysis of the model geometry was carried out with the program *PROCHECK* (*39*). The plot indicated that 90.6% of the residues were in the favorable regions and 9.4% in the allowed regions. The final *R*-factor and R_{free} of the oxidized structure for all reflections between 6.0 and 1.7 Å resolution were 0.234 and 0.255, respectively. Five percent of the reflections were set aside for R_{free} calculations (*40*). The final model of oxidized plastocyanin from *Dryopteris* is made up of one monomer per asymmetric unit with 102 amino residues, 758 protein atoms (non-hydrogen), 49 water molecules, and a single copper ion. The last cycle of the refinement gave a quite reasonable stereochemistry by using 9809 unique reflections in the range of 6.0−1.7 Å resolution. The root-mean-square (rms) deviations from standard values are 0.013 Å for bond distances (1−2 distance), 2.78 Å for angle distances (1−3 distance), and 27.4 Å for dihedral angles (planar 1−4 distance). From a Ramachandran plot, the current model is considered to exhibit good stereochemistry.

A similar procedure was applied to the refinement of the reduced structure. The reduced structure, including 38 water molecules, is refined up to 1.8 Å resolution with *R*-factor and R_{free} values of 20.7 and 22.6%, respectively. The root-mean-square deviations from ideal geometry of the bond lengths and angles were 0.014 Å and 2.89°, respectively.

Table 1: Final Refinement Statistics for the Oxidized and Reduced Plastocyanin from *D. crassirhizoma*

	oxidized form	reduced form
resolution (Å)	6.0−1.7	6.0−1.8
no. of protein atoms	758	758
no. of copper ion	1	1
no. of water molecules	49	38
no. of reflections		
working set	9809	8478
test set for R_{free}	1016	894
R (%)	23.4	20.7
R_{free} (%)	25.5	22.6
average temperature factors (A^2)		
all atoms	23.6	24.2
main chain atoms	21.4	22.0
side chain atoms	24.5	25.6
metal ions	16.4	19.5
solvent atoms	36.4	35.4
rms deviations from standard geometries		
bond lengths (Å)	0.013	0.014
bond angles (deg)	2.78	2.89
dihedral angles (deg)	27.4	27.4
improper angles (deg)	1.75	1.19
Ramachandran plot (%)		
most favored	90.6	91.8
allowed	9.4	8.2

The mean positional errors of the atoms estimated by Luzzati plots are 0.21 Å for the oxidized protein and 0.22 Å for the reduced protein (*41*). For well-defined parts of the structure, especially the β-strands, the internal side chains, and the region around the metal site, the errors are likely to be lower. Both structures have been deposited in the Protein Data Bank as 1KDJ and 1KDI, respectively. The numbering of amino residues for both forms is referenced to that of poplar plastocyanin. The results of data collection and refinement are summarized in Table 1.

RESULTS

Overall Structure. A ribbon drawing of *Dryopteris* plastocyanin is presented in Figure 1a.

The molecule has eight β-strands forming two β-sheets. β-Sheet I consists of four β-strands: S1, residues 2−5; S2a, residues 14 and 15; S3, residues 27−31; and S6, residues 69−73. β-Sheet II contains four β-strands: S2b, residues 18−21; S4, residues 40 and 41; S7, residues 78−83; and S8, residues 93−98.

Both poplar and the fern belong to the same category of higher plants. Nevertheless, the amino acid sequences are quite different from each other with a percent identity of only 35%, and the whole structure is remarkably different from those of other plastocyanins. The structure of *Dryopteris* plastocyanin has a two-and-one-half-turn α-helix from Gly47A to Ala54 instead of the conventional half-turn α-helix found in higher-plant and green algal plastocyanins.

The amino acid sequence alignment of plastocyanin from *Dryopteris*, poplar, *Ulva*, *Anabaena*, *Synechocystis*, and *Synechococcus* is shown in Figure 2.

The number of identical residues is 36/102 (35%) for *Dryopteris* and poplar, 41/102 (40%) for *Dryopteris* and *Ulva*, 33/102 (32%) for *Dryopteris* and *Anabaena*, 33/102 (32%) for *Dryopteris* and *Synechocystis*, and 28/102 (27%) for *Dryopteris* and *Synechococcus*. The replacement of the conserved Gly49 with Ala49 and the insertions of Gly45A, Gly47A, and Thr47B may have caused the significant change in forming the long α-helix of the protein.

Differences of Backbone Structures with Poplar. Despite sequence divergence among plastocyanins of the fern, higher plants, green algae, and cyanobacteria, the backbone structures are remarkably conserved except for the two-and-one-half-turn α-helix and the loop structure at the top surface (Figure 3).

The averaged rms deviation for the backbone atoms excluding the helix and the loops is 0.60 Å when the oxidized form of *Dryopteris* plastocyanin is compared with that of poplar, 0.63 Å when compared with green algal plastocyanin from *U. pertusa*, and 0.56 Å when compared with the cyanobacterium *Synechococcus* sp. PCC 7942. The green algal plastocyanins from *U. pertusa*, *Enteromorpha prolifera*, *Scenedesmus obliquus*, and *Chlamydomonas reinhardtii* are all missing the characteristic irregular swelling which is formed by amino acid residues 58−60 in the poplar form (*3*). On the other hand, three surplus amino acid residues (Gly45A, Gly47A, and Thr47B) exist between the first acidic patch (residues 42−45) and the second acidic patch (residues 59−61), which forms the two-and-one-half-turn α-helix. The largest differences are at residue Ala49 (7.0 Å), and those are caused by the formation of the long α-helix in the *Dryopteris* protein.

On the other hand, the superposition of the backbone structures of poplar and fern plastocyanins reveals that the turn structures at residues 7−11 and 63−68, and the loop structure at residues 32−36, of the fern form are remarkably different from those in poplar plastocyanin. The large differences are found at residues Glu8 (4.3 Å), Asp66 (6.8 Å), and Glu34 (4.8 Å). All these differences are located on the top surface of *Dryopteris* plastocyanin (Figure 4).

Especially, the turn structure at residues 7−11 is significantly different. The sequence of *Dryopteris* plastocyanin is not very homologous with plastocyanins from other higher plants, and those differences are remarkable at residues 1−15. The degrees of identity of amino acid residues in this region are both 4/15 (27%) between the plastocyanins from poplar and *Dryopteris* and between the plastocyanins from *Ulva* and *Dryopteris*. The unexpected residues Glu4, Asp7, Phe12, Lys13, and Tyr15 are introduced in this region. Two hydrogen bonds [$O_{\delta 2}$(Asp7)···N(Gly10) and $O_{\delta 1}$(Asp7)···OH(Tyr15)] stabilize the open turn at residues 7−11 (Figure 4). The cause of the structural differences proved to be the novel $\pi-\pi$ stacking interaction between the aromatic ring of Phe12 and residue His87 (Figure 4). The stable interaction lifts up the loop toward the copper ion, which is followed by the movement of the neighboring loops at residues 32−36 and 63−68.

There is hydrogen bonding between the carbonyl oxygen atom of Leu5 and the amido nitrogen atom of Ala33, and strand I and the loop of residues 33−39 are stabilized by the hydrogen bond in poplar plastocyanin. However, the $\pi-\pi$ stacking interaction moves strand I toward Phe12 and breaks the hydrogen bond between strand I and the loop of residues 33−39 in *Dryopteris* plastocyanin. Moreover, the $\pi-\pi$ interaction affects the locations of copper ion and His37 with respect to Phe12 and yields some conformational differences in residues 32−36. Gly36 is introduced in *Dryopteris* plastocyanin instead of the conserved residue Pro36. The C_α

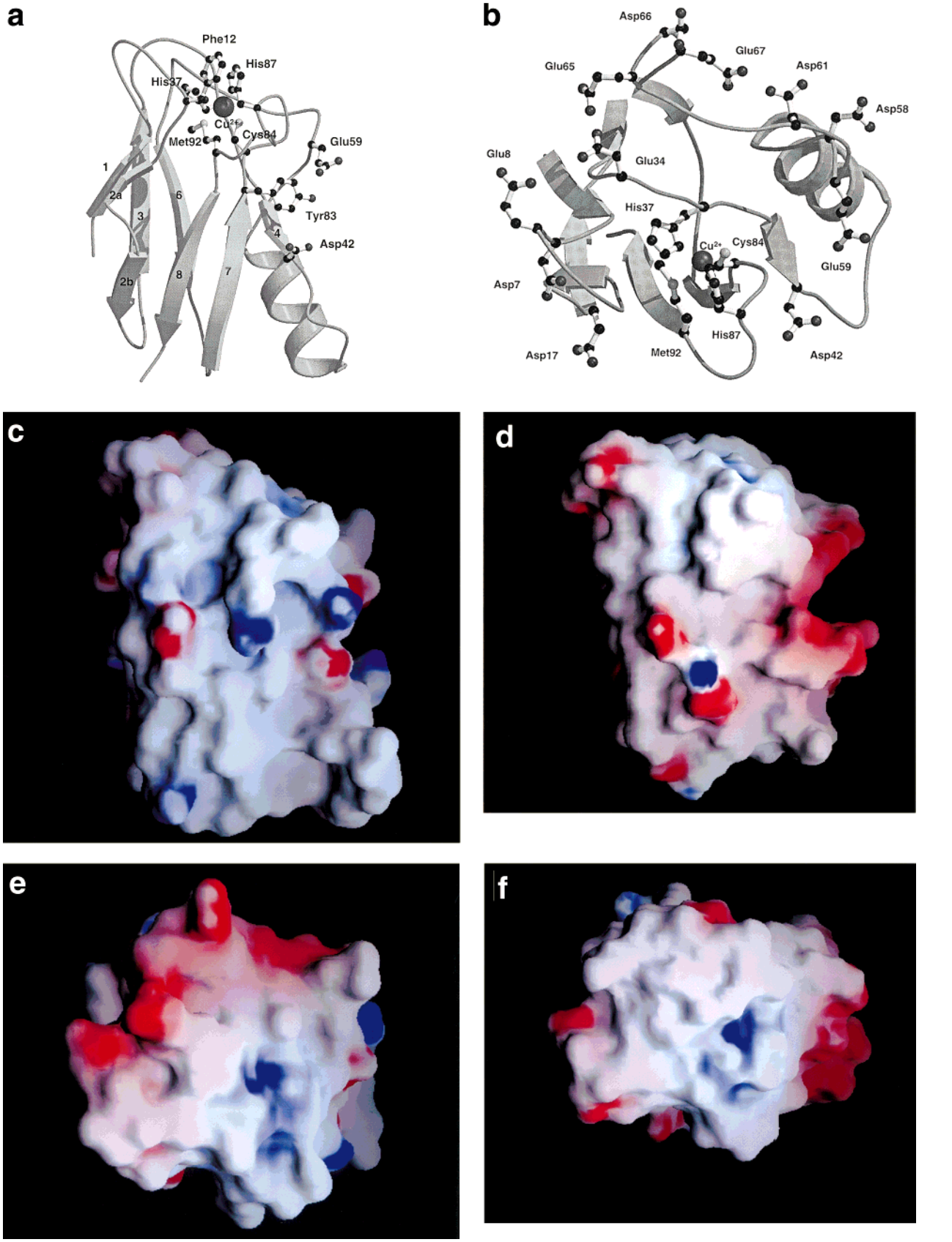

FIGURE 1: (a and b) Ribbon representation of the oxidized plastocyanin from *D. crassirhizoma* viewed from the side of the molecule (a) and from the top of the molecule (b), drawn using *MOLSCRIPT* (*46*) and *RASTER3D* (*47*). The copper ion is shown as a sphere at the top of the model. The four ligands, His37, Cys84, His87, and Met92, and Tyr83 and Phe12 are shown as ball-and-stick representations. Two acidic residues, Asp42 and Glu59, are also shown as ball-and-stick representations. *Dryopteris* plastocyanin has the two-and-one-half-turn α-helix at positions 47A−54, and it is the longest α-helix found in plastocyanins. Eleven of fifteen acidic residues are located at the top surface of the molecule. (c−f) The electrostatic potential mapping of the molecular surface of plastocyanin from *Dryopteris* (c and e) and poplar (d and f) viewed from the side and from the top of the molecule, respectively. The protein molecule is shown as a solid surface, colored according to the calculated electrostatic potential and contoured from −15 (intense red) to +15 kT/e (intense blue). Panels c−f were drawn using *GRASP* (*42*).

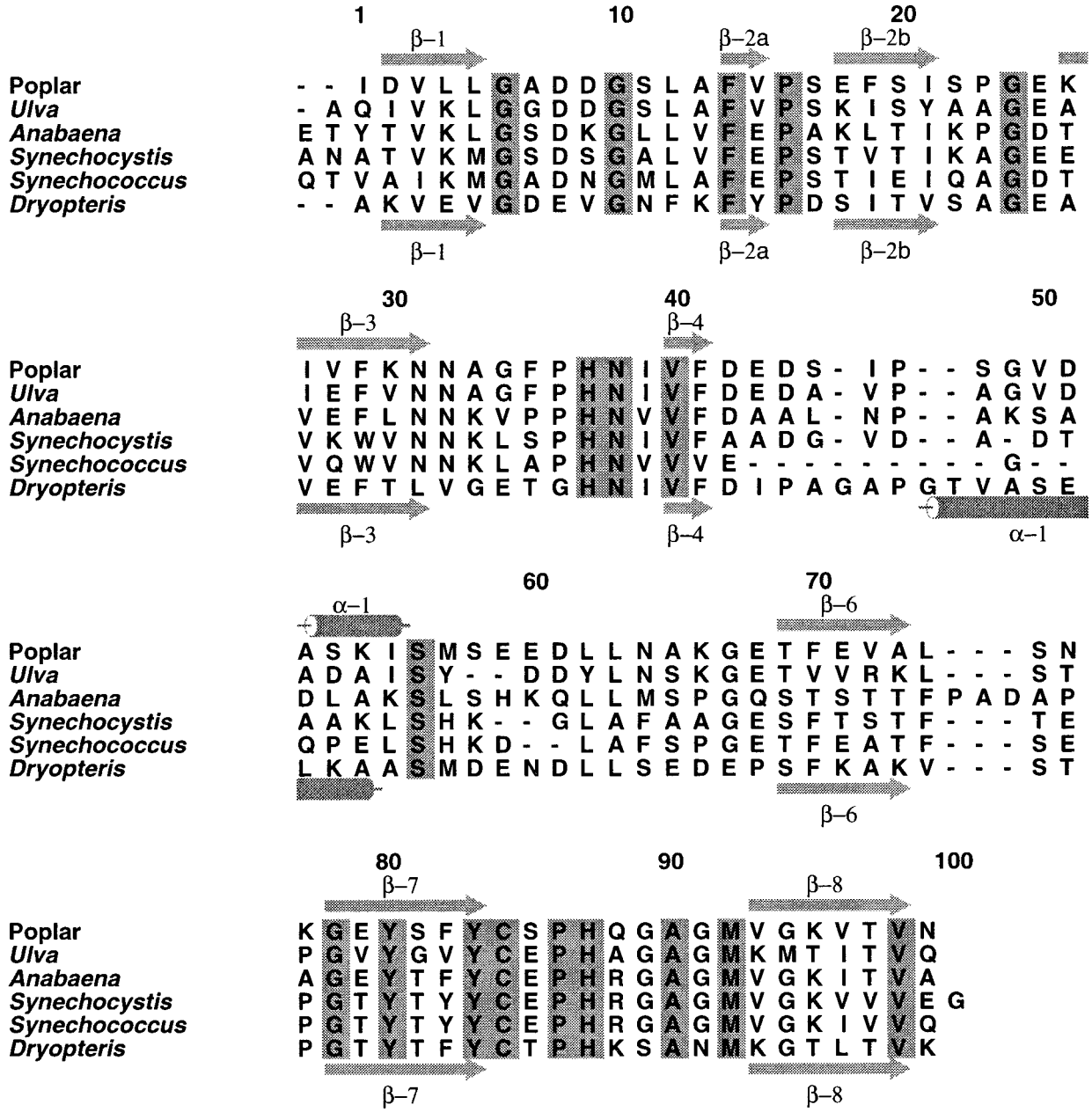

FIGURE 2: Amino acid sequence alignment of plastocyanins from the fern *D. crassirhizoma* (*24*), the seed plant poplar (plastocyanin *a*), the green algae *U. pertusa*, and cyanobacteria *A. variabilis*, *Synechocystis* sp. PCC 6803, and *Synechococcus* sp. PCC 7942, drawn using *ALSCRIPT* (*48*). Amino acid sequence data were obtained from the SWISS-PROT database. Invariant residues in all plastocyanins are shown in gray. Secondary structural elements in *Dryopteris* plastocyanin are also indicated. α-1 indicates the two-and-one-half-turn α-helix found in the *Dryopteris* protein from residues 47A to 54, while eukaryotic plastocyanins have a conventional α-helix from residues 52 to 55. The numbering of residues is like that of poplar plastocyanin.

atom of Glu34 has moved by 4.8 Å due to the flexibility of Gly36.

On the other hand, the residue at position 68 is conserved as glutamate in all other plastocyanins, but the replacement of amino acid residue Glu68 with Pro in *Dryopteris* plastocyanin and the remarkable structural change occur around the turn structure of residues 63−68.

Acidic Patch of Dryopteris Plastocyanin. The acidic patch, which is proposed to be important for docking with physiological redox partners, consists of two acidic clusters from residues 42 to 44 and 59 to 61 in higher-plant plastocyanins (*2*, *25*, *26*). However, *Dryopteris* plastocyanin has only two acidic amino acid residues, Asp42 and Glu59, around Tyr83. The total negative charge of −7, calculated from the amino acid residues, is similar to that for poplar plastocyanin. While the acidic patch is found around Tyr83 in poplar plastocyanin, the acidic residues are located around the top surface in *Dryopteris* plastocyanin. Eleven out of fifteen acidic residues, Asp7, Glu8, Asp17, Glu34, Asp42, Asp58, Glu59, Asp61, Glu65, Asp66, and Glu67, surround the hydrophobic patch like a quite huge "acidic arc". The water-accessible His87 is located at the center of the acidic arc (Figure 1b).

The surface character is apparently changed in the protein. Panels c and d of Figure 1 drawn with *GRASP* (*42*) are remarkable, since the acidic patch at the east side is quite different from that of poplar plastocyanin.

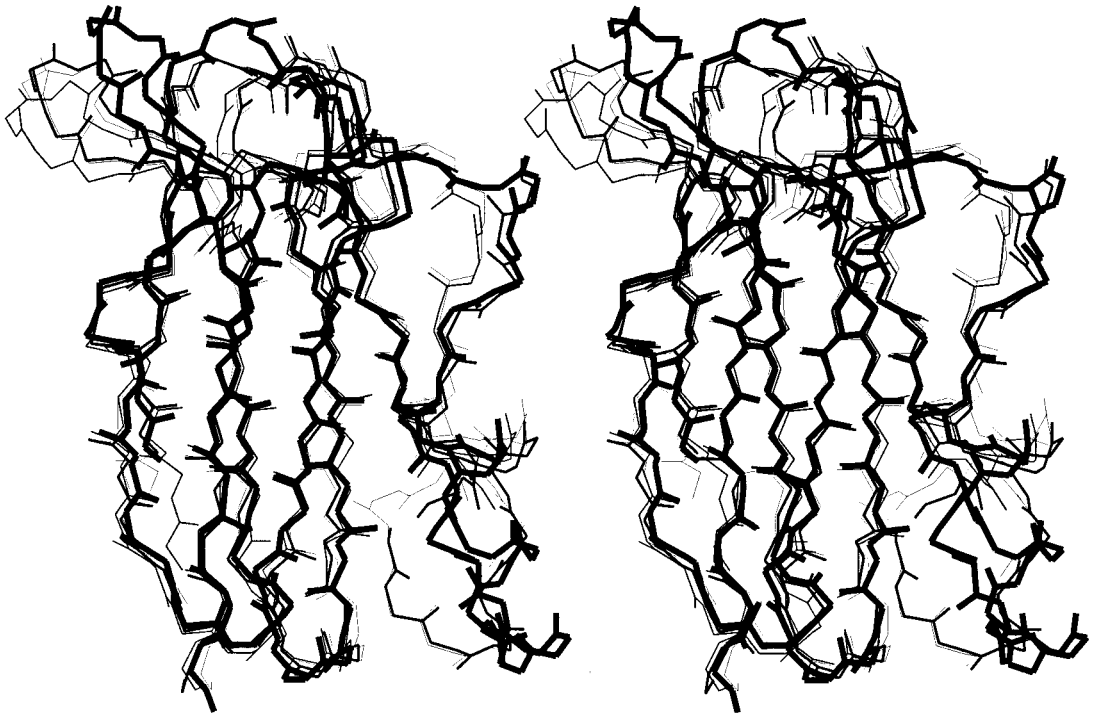

FIGURE 3: Stereoview of the backbone structure of *Dryopteris* plastocyanin (thickest lines) superimposed on the seed plant plastocyanin from poplar (second-thickest lines), the green algal plastocyanin from *U. pertusa* (third-thickest lines), and the cyanobacterial plastocyanin from *Synechococcus* sp. PCC 7942 (thin lines).

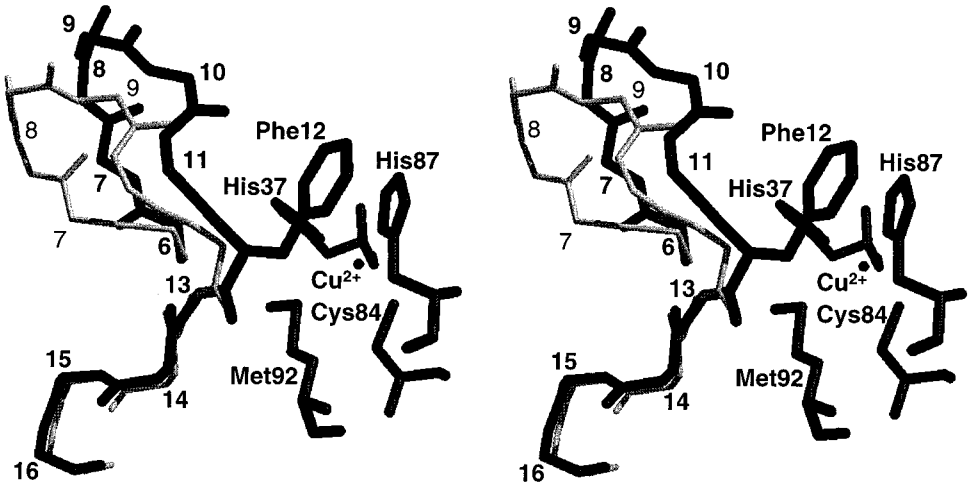

FIGURE 4: Stereoview of the backbone structures at the top surface between *Dryopteris* and poplar plastocyanins. Remarkable differences are found at residues 7−11. The $\pi-\pi$ stacking interaction between Phe12 and His87 withdraws the loop structure of residues 7−11 and makes the large structural changes at the top surface of the molecule, which is followed by the movement of the neighboring loops of residues 32−36 and 63−68.

On the other hand, the hydrophobic patch of the *Dryopteris* protein is surrounded by the huge acidic arc, and the electrostatic character of the top surface is also remarkable (panels e and f of Figure 1).

Pseudoazurin and azurin have the similar basic ring formed by amino acid residues lysine, arginine, and histidine (*43*), some of which are quite important for the recognition of the physiological electron acceptor.

Copper Structure and the Change upon Reduction. The copper geometry is a distorted tetrahedral structure like other plastocyanins (Table 2).

The distance parameters of the copper geometry are 1.99 Å for Cu−N(His37), 2.23 Å for Cu−S(Cys84), 2.06 Å for Cu−N(His87), and 2.94 Å for Cu−N(Met92). A slightly longer Cu−S(Cys84) bond is seen, compared with those of other plastocyanins. The angle parameters of copper ligands are similar to those in other plastocyanins. However, the reduced *Dryopteris* plastocyanin exhibits the almost same parameters as the oxidized molecule for the copper coordination structure. The copper coordination structure is quite stable upon reduction at pH 4.5 (Table 2), which is quite different from the case with all other plastocyanins. Phe12 replaces conserved residue Leu12 in *Dryopteris* plastocyanin, and it is located in the neighborhood of the ligand His87 with a distance of 3.5 Å. Apparently, there is a $\pi-\pi$ stacking interaction between the ligand histidine and the aromatic ring

Table 2: Bond Lengths and Bond Angles of Copper Structures in Plastocyanins

	fern *D. crassirhizoma*		seed plant poplar			green alga *U. pertusa*		cyanobacterium *Synechococcus* sp.	
	oxidized pH 4.5	reduced pH 4.5	oxidized pH 6.0	reduced pH 3.8	reduced pH 7.0	oxidized pH 6.0	reduced pH 6.0	oxidized pH 5.0	reduced pH 5.0
bond lengths (Å)									
Cu−N(His37)	1.99	1.95	1.91	2.12	2.12	2.08	2.02	1.97	2.09
Cu−N(His87)	2.06	2.10	2.06	3.12	2.39	2.06	2.07	2.01	2.37
Cu−S(Cys84)	2.23	2.21	2.07	2.13	2.16	2.18	2.18	2.14	2.17
Cu−S(Met92)	2.94	2.91	2.82	2.51	2.87	2.69	2.63	2.93	2.80
bond angles (deg)									
N(His37)−Cu−N(His87)	105.9	104.6	97.2	88.3	99.07	96.2	95.3	101.4	93.4
N(His37)−Cu−S(Cys84)	128.4	130.1	131.7	140.6	136.3	133.0	136.3	131.0	140.3
N(His37)−Cu−S(Met92)	81.0	80.9	88.5	95.0	87.9	89.5	88.5	86.0	91.9
N(His87)−Cu−S(Cys84)	118.8	117.3	121.0	87.2	109.8	115.3	111.8	121.4	108.5
N(His87)−Cu−S(Met92)	107.8	108.4	100.6	106.4	106.0	104.6	108.8	98.8	99.9
S(Cys84)−Cu−S(Met92)	106.5	108.2	109.9	123.7	113.4	113.0	112.4	107.7	115.4

of Phe12 (Figure 1a). The copper ligand His37 was prevented from being protonated upon reduction at low pH in *Dryopteris* plastocyanin. The ability of the protein to remain active at low pH, unexpected absorption spectra, and the high redox potential have recently been reported (*24*).

Redox-Induced Conformational Changes around the Copper Site. The rms deviation of the backbone structures between the two oxidation states of the protein is just 0.16 Å. When all atoms are included in the calculation, the rms deviation between the two structures is 0.79 Å. However, the errors are lower for well-defined parts of the structure, especially the β-strands, the internal side chains, and the region around the metal site. The $\pi-\pi$ stacking interaction between Phe12 and the water-accessible ligand His87 has been shown to protect the protonation and rotation of the ligand histidine. However, we have confirmed the large conformational change of residue Glu59 upon reduction. In the oxidized structure, the $O_{\epsilon 1}$ atom of Glu59 hydrogen bonds to the OH of Tyr83 with the distance being 3.1 Å. However, the $O_{\epsilon 1}$ atom of Glu59 moves away from the OH of Tyr83 with the distance being 11.3 Å after reduction.

The movement of Glu59 was also confirmed in poplar plastocyanin upon reduction at pH 7.0 (*12*). Because both vascular plant plastocyanins show the movement of Glu59 upon reduction, the phenomena suggest the important role of Glu59. Another movement upon reduction is found around the $\pi-\pi$ stacking structure formed between His87 and Phe12. The next residue of Lys13 flips in the oxidized state; however, in the reduced state, the N_ζ atom of Lys13 moves to approach a water molecule, which is hydrogen bonded to the OH of Tyr15. The redox potential was raised by 20 mV compared to those of other higher-plant plastocyanins by the $\pi-\pi$ stacking interaction between His87 and Phe12 (*24*). The $\pi-\pi$ stacking interaction apparently influences the character of copper ion. The reduction of copper ion may have an effect on Phe12. The movement of Lys13 may suggest that the influence is spread toward Tyr15.

DISCUSSION

The structure determinations of the oxidized plastocyanin from the fern *D. crassirhizoma* revealed that the protein possesses a two-and-one-half-turn α-helix instead of the conventional α-helix found in all eukaryote plastocyanins. *Dryopteris* plastocyanin is comprised of the highest number of amino acid residues (102) of any known higher-plant plastocyanins. The alignment of the primary structures of the plastocyanins (Figure 2) shows the large sequence differences around the acidic patch in *Dryopteris* plastocyanin and the cyanobacterial proteins, as compared to their algal and higher-plant counterparts. All plastocyanins from green algae and higher plants have Gly49 at their half-turn helix. In the cyanobacterial plastocyanin from *Synechocystis*, Gly49 is lacking and the α-helix extends from Asp47 to Lys54, resulting in a complete two-turn helix (*22*). In *Anabaena* plastocyanin, a lysine residue is found at residue 49 and the two-turn helix is formed (*21*). *Dryopteris* plastocyanin has an alanine at residue 49, and has a three-amino acid insertion before Ala49 (*24*). The backbone structures of plastocyanins differ dramatically from each other in the vicinity of the helix due to the replacements, insertions, or deletions of amino acids around residue 49.

In higher-plant plastocyanins, the conserved residues at positions 42−44 and 59−61 form the acidic patch around Tyr83, which is believed to be important for the recognition of electron transfer partners. However, only two acidic residues are found around Tyr83 in cyanobacterial plastocyanins, namely, Glu42 and Asp59. On the other hand, the green algal plastocyanins are all missing the second acidic patch consisting of residues 58−60 (*3*). In *Dryopteris* plastocyanin, three extra amino acid residues exist between the first acidic patch (residues 42−45) and the second acidic patch (residues 59−61), which forms the two-and-one-half-turn α-helix. Most of the acidic residues in the acidic clusters are conserved in the protein; however, the location of the second acidic cluster is changed in *Dryopteris* plastocyanin. Alternatively, it could be argued that the formation of the two-and-one-half-turn α-helix moves both of the acidic clusters, since *Dryopteris* plastocyanin possesses two acidic clusters at residues 59−61 and 65−67, instead. As the result, the distribution of the acidic charge is quite unique in the protein (panels b and e of Figure 1). These results provide a novel insight into the molecular evolutional interest.

The copper coordinational structure of *Dryopteris* plastocyanin is not changed when the protein is reduced at even the low pH of 4.5. The $\pi-\pi$ stacking interaction between Phe12 and the water-accessible ligand His87 found in *Dryopteris* plastocyanin has proved to protect the protonation and rotation of the ligand histidine. The detailed correlation between the $\pi-\pi$ structure and the functions was previously reported by Kohzuma et al. From the investigation of the pH dependency of the rate constants for the reaction with $[Fe(CN)_6]^{3-}$ or $[Co(phen)_3]^{3+}$ complexes, the acid dissocia-

tion constants accompanying the reaction with $[Fe(CN)_6]^{3-}$ and $[Co(phen)_3]^{3+}$ were determined to be 5.9 ± 0.1 and 6.2 ± 0.3, respectively (*24*). Sykes suggested that the pK_H values obtained from the kinetic experiments using $[Co(phen)_3]^{3+}$ are due to the contribution arising from both the acidic patch and the active site protonation (*44*). The structural studies show the apparent protection of protonation at the active site, which suggests that *Dryopteris* plastocyanin would reflect the pure protonation process at the acidic patch. A small but significant conformational change occurs at Glu59 upon reduction in *Dryopteris* plastocyanin, together with the movement of residue Lys13. On the other hand, the movement of Glu59 upon reduction was also observed in poplar plastocyanin at pH 7.0. The fact that both Glu59 and Lys13 are located ca. 12 Å from the copper ion is quite interesting. Tyr83 in the oxidized structure should carry a proton. In the oxidized form, the hydrogen bond between Tyr83 and Glu59 implies that Tyr83 must be acting as a proton donor. From the results of the movements about Glu59 found in both poplar and *Dryopteris* plastocyanins, the distribution of minus charge from the Cu(I) ion to Tyr83 may occur upon reduction.

Most of the acidic residues are unique in *Dryopteris* plastocyanin. Moreover, the large arc made by 11 out of 15 acidic residues is quite remarkable in the protein, since the arc surrounds the hydrophobic patch. Both the hydrophobic patch around the $\pi-\pi$ stacking structure and the acidic arc may have important roles in the recognition of photosystem I or cytochrome b_6−cytochrome *f* complex. However, the electron transfer mechanism for transfer between *Dryopteris* plastocyanin and cytochrome *f* may be similar to that in other higher plants, since the hydrogen bond between Glu59 and Tyr83 is conserved in the oxidized protein and residue Glu59 is flipped away from Tyr83 upon reduction like in poplar plastocyanin.

There are many residues that are quite unique in the fern plastocyanin. They are Phe12, Leu31, Val32, Glu34, Thr35, Gly36, Ala49, Ala55, Ser64, Glu67, Pro68, Phe70, Lys88, Ser89, and Asn91. These amino acid residues are conserved in other eukaryote plastocyanins as Leu12, Asn31, Asn32, Gly34, Phe35, Pro36, Gly49, Ile55, Asn64, Gly67, Glu68, Tyr70, Gln88, Gly89, and Gly91. Gly36 and Pro71 in *Dryopteris* plastocyanin are concerned with the structural changes. The carbonyl oxygen of Gly36, located 4.0 Å from the copper atom, is particularly interesting. Gly36 is one of the most unique residues in plastocyanins, since the location of Gly36 corresponds to that of Gly45 in azurin, in which the copper coordinational structure is trigonal bipyramidal due to flexible residue Gly45 (*45*). The highly conserved residues in higher-plant plastocyanins are indeed replaced in *Dryopteris* plastocyanin.

ACKNOWLEDGMENT

We thank Professor N. Sakabe of Tsukuba University (Tsukuba, Japan) and Drs. N. Watanabe, M. Suzuki, and N. Igarashi of the National Laboratory for High Energy Physics for kind help in data collection at Photon Factory.

REFERENCES

1. Haehnel, W. (1986) *Encyclopedia of Plant Physiology*, Vol. 19, pp 547−559, Springer, Berlin.
2. Gross, E. L. (1993) *Photosynth. Res. 37*, 103−116.
3. Redinbo, M. R., Yeates, T. O., and Merchant, S. (1994) *J. Bioenerg. Biomembr. 26*, 49−66.
4. Sandmann, G., Reck, H., Kessler, E., and Böger, P. (1983) *Arch. Microbiol. 134*, 23−27.
5. Wood, P. M. (1978) *Eur. J. Biochem. 87*, 9−19.
6. Merchant, S., and Bogorad, L. (1986) *Mol. Cell. Biol. 6*, 462−469.
7. Sandmann, G. (1986) *Arch. Microbiol. 145*, 76−79.
8. Bovy, A., de Vrieze, G., Borrias, M., and Weisbeek, P. (1992) *Mol. Microbiol. 6*, 1507−1513.
9. Zhang, L., McSpadden, B., Pakrasi, H. B., and Whitmarsh, J. (1992) *J. Biol. Chem. 267*, 19054−19059.
10. Colman, P. M., Freeman, H. C., Guss, J. M., Murata, M., Norris, V. A., Ramshaw, J. A. M., and Venkatappa, M. P. (1978) *Nature 272*, 319−324.
11. Guss, J. M., and Freeman, H. C. (1983) *J. Mol. Biol. 169*, 521−563.
12. Guss, J. M., Harrowell, P. R., Murata, M., Norris, V. A., and Freeman, H. C. (1986) *J. Mol. Biol. 192*, 361−387.
13. Moore, J. M., Case, D. A., Chazin, W. J., Gippert, G. P., Havel, T. F., Powls, R., and Wright, P. E. (1988) *Science 240*, 314−317.
14. Bagby, S., Driscoll, P. C., Goodall, K. G., Redfield, C., and Hill, H. A. O. (1990) *Eur. J. Biochem. 188*, 413−420.
15. Moore, J. M., Lepre, C. A., Gippert, G. P., Chazin, W. J., Case, D. A., and Wright, P. E. (1991) *J. Mol. Biol. 221*, 533−555.
16. Collyer, C. A., Guss, J. M., Sugimura, Y., Yoshizaki, F., and Freeman, H. C. (1990) *J. Mol. Biol. 211*, 617−632.
17. Redinbo, M. R., Cascio, D., Choukair, M. K., Rice, D., Merchant, S., and Yeates, T. O. (1993) *Biochemistry 32*, 10560−10567.
18. Bagby, S., Driscoll, P. C., Harvey, T. S., and Hill, H. A. O. (1994) *Biochemistry 33*, 6611−6622.
19. Sugawara, H., Inoue, T., Li, C., Gotowda, M., Hibino, T., Takabe, T., and Kai, Y. (1999) *J. Biochem. 125*, 899−903.
20. Shibata, N., Inoue, T., Nagano, C., Onodera, K., Yoshizaki, F., Sugimura, Y., and Kai, Y. (1998) *J. Biol. Chem. 274*, 4225−4230.
21. Badsberg, U., Jørgensen, A. M. M., Gesmar, H., Led, J. J., Hammerstad, J. M., Jespersen, L.-L., and Ulstrup, J. (1996) *Biochemistry 35*, 7021−7031.
22. Romero, A., De la Cerda, B., Varela, P. F., Navarro, J. A., Hervás, M., and De la Rosa, M. A. (1998) *J. Mol. Biol. 275*, 327−336.
23. Inoue, T., Sugawara, H., Hamanaka, S., Tsukui, H., Suzuki, E., Kohzuma, T., and Kai, Y. (1999) *Biochemistry 38*, 6063−6069.
24. Kohzuma, T., Inoue, T., Yoshizaki, F., Sasakawa, Y., Onodera, K., Nagatomo, S., Kitagawa, T., Uzawa, S., Isobe, Y., Sugimura, Y., Gotowda, M., and Kai, Y. (1999) *J. Biol. Chem. 274*, 11817−11823.
25. Sykes, A. G. (1985) *Chem. Soc. Rev. 14*, 283−315.
26. Sykes, A. G. (1991) *Adv. Inorg. Chem. 36*, 377−408.
27. Gross, E. L. (1993) *Photosynth. Res. 37*, 103−116.
28. Navarro, J. M., Hervás, M., and De la Rosa, M. A. (1997) *JBIC, J. Biol. Inorg. Chem. 2*, 11−22.
29. Vakoufari, E., Wilson, K. S., and Petratos, K. (1994) *FEBS Lett. 347*, 203−206.
30. Zhu, Z., Cunane, L. M., Chen, Z., Durley, R. C. E., Mathews, F. S., and Davidson, V. L. (1998) *Biochemistry 37*, 17128−17136.
31. Sakabe, N. (1991). *Nucl. Instrum. Methods Phys. Res. A303*, 448−463.
32. Otwinowski, Z. (1993) *Proceedings of CCP4 Study Weekend* (Sawyer, L., Issacs, N., and Bailey, S., Eds.) pp 56−62, Daresbury Laboratory, Warrington, U.K.
33. Navaza, J. (1994) *Acta Crystallogr. A50*, 157−163.
34. Collaborative Computational Project, Number 4 (1994) *Acta Crystallogr. D50*, 760−763.
35. Guss, J. M., Bartunik, H. D., and Freeman, H. C. (1992) *Acta Crystallogr. B48*, 790−811.

36. Brünger, A. T., Kurian, J., and Karplus, M. (1987) *Science 235*, 458−460.
37. Jones, T. A. (1978) *J. Appl. Crystallogr. 15*, 23−31.
38. Ramachandran, G. N., and Sasisekharan, V. (1968) *Adv. Protein Chem. 23*, 283−437.
39. Laskowski, R. A., MacArthur, M. W., Moss, D. S., and Thornton, J. M. (1993) *J. Appl. Crystallogr. 26*, 283−291.
40. Brünger, A. T. (1992) *Nature 355*, 472−474.
41. Luzzati, V. (1952) *Acta Crystallogr. A5*, 802−810.
42. Nicholls, A., Bharadwaj, R., and Honig, B. (1993) *Biophys. J. 64*, A166.
43. Kukimoto, M., Nishiyama, M., Ohnuki, T., Turley, S., Adman, E. T., Horinouchi, S., and Beppu, T. (1995) *Protein Eng. 8*, 153−158.
44. Sykes, A. G. (1990) *Struct. Bonding 75*, 175−224.
45. Baker, E. N. (1988) *J. Mol. Biol. 203*, 1071−1095.
46. Kraulis, P. J. (1991) *J. Appl. Crystallogr. 24*, 946−950.
47. Merrit, E. A., and Murphy, M. E. (1994) *Acta Crystallogr. D50*, 869−873.
48. Barton, G. J. (1993) *Protein Eng. 6*, 37−40.

BI990502T